Int. J. Electrochem. Sci., 10 **(2015)** 9192 - 9204

International Journal of ELECTROCHEMICAL SCIENCE
www.electrochemsci.org

Multi-walled Carbon Nanotubes-Aminate Reduced Graphene Oxide Modified Glassy Carbon Electrode as the Voltammetric Sensor for Sensitive Electrochemical Determination of Rutin

Xiaofei Zhu[1,2,†], *Jingkun Xu*[1,†], *Xuemin Duan*[1,*], *Limin Lu*[2,*], *Huakun Xing*[1], *Yansha Gao*[1], *Hui Sun*[1], *Liqi Dong*[1], *Taotao Yang*[1]

[1]School of Pharmacy, Jiangxi Science and Technology Normal University, Nanchang 330013, PR China
[2]College of Science, Jiangxi Agricultural University, Nanchang 330045, PR China
[†] These authors contributed equally to this work and should be considered co-first authors.
[*]E-mail: duanxuemin@126.com, lulimin816@hotmail.com

Received: 24 August 2015 / *Accepted:* 10 September 2015 / *Published:* 30 September 2015

In this paper, a highly sensitive voltammetric method for determination of rutin is developed using multi-walled carbon nanotubes-aminate reduced graphene oxide (MWCNTs/ARGO) modified electrode. The incorporated ARGO served as dispersing agent and conductive sheet, which could effectively prevented aggregation of MWCNTs. Compared with either MWCNTs or ARGO, the hybrid nanomaterials showed a strong synergistic effect between two materials and exhibited higher activity for the electro-oxidation of rutin. MWCNTs/ARGO composite was characterized by scanning electron microscope (SEM) and electrochemical impedance spectroscopy (EIS). Under the optimized conditions, MWCNTs/ARGO modified electrode exhibited wide linear range from 0.01 to 112 μM with the detection limit of 2 nM (S/N = 3). Moreover, the proposed method was successfully applied to determine rutin in compound rutin tablets and satisfactory results were obtained.

Keywords: Rutin; Graphene oxide; Carbon nanotubes; Determination; Sensor

1. INTRODUCTION

Rutin (3',4', 5, 7-tetrahydroxyflavone 3β-D-rutinoside) is a kind of bioactive flavonoid glycosides, which is often used as anti-tumor, anti-inflammatory, anti-oxidants, etc. It is also used as a therapeutical medicine with the functions in a wide range of circulatory problems, which can lower blood pressure, reduce capillary permeability and dilute the blood [1]. Therefore, develop simple and sensitive methods for rutin determination is very important.

Up to date, different methods have been reported for the determination of rutin, including high-performance liquid chro-matography (HPLC) [2], UV–vis spectrophotometry [3], capillary

electrophoresis (CE) [4], flow injection analysis (FIA) [5], sequential injection analysis [6] and electrochemical methods [7-9]. Among these methods, electrochemical methods have the advantages such as simple, fast, sensitive and reliable. Electrochemical sensors also can be fabricated with small dimensions and suitable for placement directly into biological samples. Based on the electroactivity of rutin, it has been investigated and determined by electrochemical methods. Kang et al. [10] used glassy carbon electrode (GCE) for rutin determination and further applied to real samples analysis. Zeng et al. [11] investigated the detection of rutin at a single-walled carbon nanotubes modified gold electrode and obtained a better sensitivity for rutin. Wei et al. [12] fabricated a CeO_2 nanoparticle-modified electrode for rutin determination and demonstrated a strong catalytic effect of nanoparticle towards electrochemical oxidation of rutin. Due to the presence of modifier on the electrode surface, electrochemical behaviours of rutin and sensitivity can be greatly enhanced.

Carbon nanotubes (CNTs) have received extensive attention due to their nanoscale dimensions and outstanding materials properties including ballistic electronic conduction, immunity from electromigration effects at high current densities, and transparent conduction [13-15]. The applications of CNTs have been reported in various fields such as batteries [16], supercapacitors [17], chemical sensors and biosensors [18, 19]. However, due to Van der Waals interactions between the side walls, CNTs tend to irreversible agglomeration in a short period of time. These disadvantages seriously limit the applications of CNTs and CNTs-based materials in many fields. To overcome this shortcoming, different methods were invented for the dispersion of CNTs, including chemical oxidation [20,21] and the use of surfactants [22-24] or metal salts [25,26]. However, strong acids treatment results in material degradation and reduction of the electronic, thermal and mechanical properties [27-29]. While the use of surfactants can not obtain stability CNTs suspension in wide concentration rang, and adding of metal salts would reduce the stability of suspension, as the DLVO theory predicted [32]. It has been reported CNTs can be well dispersed through the introduction of graphene and its derivatives and the obtained hybrid material exhibited better properties compared with individual component [33,34].

In this work, MWCNTs/ARGO nanocomposite was prepared using a simple ultrasonic mixing method. ARGO served as dispersant which can effectively prevent agglomeration of MWCNTs without reducing their superior properties. In addition, due to the excellent conductivity and large surface area of rGNC, MWCNTs/ARGO modified GCE exhibited better performance towards electro-oxidation of rutin as compared to MWCNTs modified GCE. Consequently, an electrochemical sensor based on MWCNTs/ARGO modified electrode was developed for the determination of rutin. The sensor presents high sensitivity, low limits of detection, and excellent selectivity, which can open up new opportunities for sensitivity, simple and sensitive detection of rutin in real sample analysis.

2. EXPERIMENTAL

2.1. Chemicals and reagents

Rutin was obtained from Biopurify and ARGO was purchased from Nanjing Xianfeng nano Co. MWCNTs (purity > 95 %) were obtained from Shenzhen Nanotech Port Co. Ltd. Rutin stock solution (5×10^{-3} M) was prepared in absolute ethanol and stored at 277~281 K. Lithium perchlorate trihydrate ($LiClO_4•3H_2O$), acetic acid, disodium hydrogenphosphate dodecahydrate (Na_2HPO_4), and

sodium dihydrogenphosphate dehydrate (NaH_2PO_4) were obtained from Sinopharm chemical reagent Co. Ltd. Al reagents were of analytical grade unless specific instructions. Redistilled water was used during the experiments.

2.2. Apparatus

Electrochemical measurements were carried out on a CHI 660D electrochemical workstation (Shanghai, China). The measurement was carried out in a three-electrode system, including glass carbon electrode (GCE) or composites modified GCE as working electrode, platinum wire as auxiliary electrode and saturated calomel reference electrode (SCE). During the experiments, the atmosphere of redistilled water was set by passing N_2 for 15 min. Except the specific statement, the electrochemical measurements were carried out in 0.1 M PBS (pH 7) at room temperature (25 ± 4 ◦C).

2.3. Preparation of MWCNTs/ARGO and fabrication of MWCNTs/ARGO /GCE

The MWCNTs/ARGO suspension was prepared by adding 2 mg ARGO and 1 mg pristine MWCNTs to 1 ml deionized water. A stable black suspension was obtained by ultrasonicating for 2 h. Prior to modification, GCE was polished with chamois leather containing 0.05 μm Al_2O_3, then cleaned by ultrasonically with doubly-distilled, absolute ethanol and redistilled water, respectively, each for 5 min. To obtain MWCNTs/ARGO modified GCE (MWCNTs/ARGO/GCE), 5 μL MWCNTs/ARGO dispersion was dropped on GCE and dried (at room temperature). For comparison, the MWCNTs modified GCE (MWCNTs/GCE), ARGO modified GCE (ARGO/GCE) were also prepared.

3. RESULTS AND DISCUSSION

3.1. Characterization of the synthesized MWCNTs/ARGO*/GCE*

The morphologies of the prepared ARGO, MWCNTs and MWCNTs/ARGO were investigated by means of SEM (**Fig. 1**). It was found that ARGO exhibited crumpled and wrinkled flake like morphology (A), while large quantities of MWCNTs were well distributed within the film and displayed serious aggregation problem (B). However, one can see that the extent of aggregation and number of junctions between MWCNTs in MWCNTs/ARGO (C) hybrid film were clearly reduced compared to raw MWCNTs, which can be attribute to the excellent dispersing ability of ARGO. The uniformly distributed MWCNTs/ARGO nanohybrid can greatly improved conductivity and increase the surface-to-volume ratio and be highly efficient to capture more rutin molecules, thus the response properties of the prepared sensors will be greatly improved.

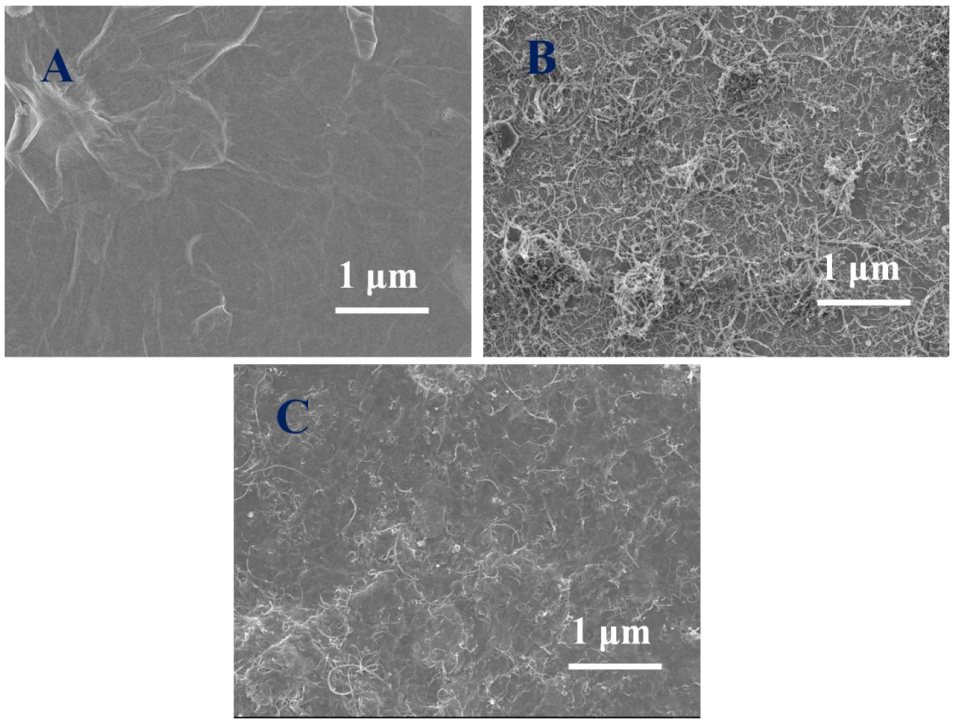

Figure 1. SEM images of ARGO (A), MWCNTs (B) and MWCNT/ARGO (C).

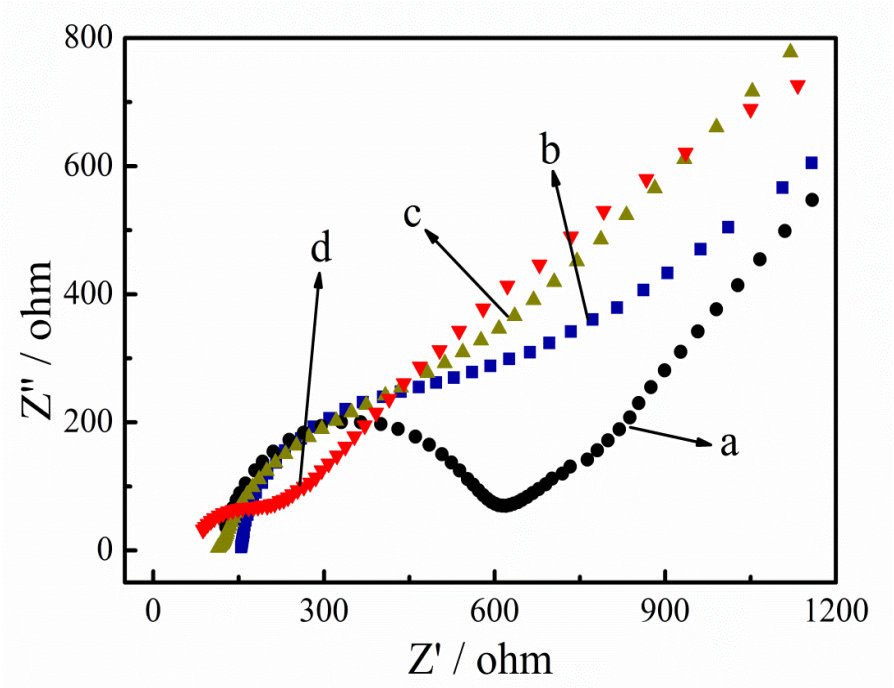

Figure 2. The electrochemical impedance spectrum of GCE (a), MWCNTs/GCE (b), ARGO/GCE (c) and MWNTs/ARGO/GCE (d) in 5 mM $Fe(CN)_6^{3-/4-}$ (1:1) solution containing 0.1 M KCl.

In order to study the interface properties of modified electrodes, electrochemical impedance spectrum (EIS) technique was used to characterization of graphene-related materials. EIS curve usually consists two parts, a semicircle part at high frequency corresponding to electron transfer resistance

(R_{et}) and straight part at low frequency corresponding to diffusion process. **Fig. 2** displays the EIS curves of bare GCE (a), MWCNTs/GCE (b), ARGO/GCE (c), and MWCNTs/ARGO/GCE (d). It can be observed that the R_{et} of bare GCE was 600 Ω, while MWCNTs/GCE showed a R_{et} of 300 Ω. When ARGO was modified on GCE, the R_{et} decreased again, indicating the excellent conductivity of ARGO. Smallest R_{et} value can be observed on MWCNTs/ARGO/GCE, which was attributed to the fact ARGO prevented the aggregation of MWCNTs as well as the synergistic effect between MWCNTs and ARGO.

*3.2 Electrochemical behavior of rutin on MWCNTs/*ARGO*/GCE*

Cyclic voltammetric responses of rutin at the bare GCE (a), MWCNTs/GCE (b), ARGO/GCE (c) and MWCNTs/ARGO/GCE (d) in the presence of 30 μM rutin (0.1 M PBS, pH 7.0) were shown in **Fig. 3**. As can be seen, no obvious peak can be found at bare GCE, which might be due to the sluggish electron transfer of low conductivity of GCE. At MWCNTs/GCE and ARGO/GCE, the redox peak currents increased significantly, which were clear evidences of strong interfacial accumulation abilities of MWCNTs and excellent conductivity of ARGO. Morever, the peak current increased again at MWCNTs/ARGO/GCE due to the synergistic effect of MWCNTs and ARGO, in which the uniformly distributed MWCNTs improved accumulation ability and ARGO sheets provided a large specific surface area to increase the loading amount of rutin.

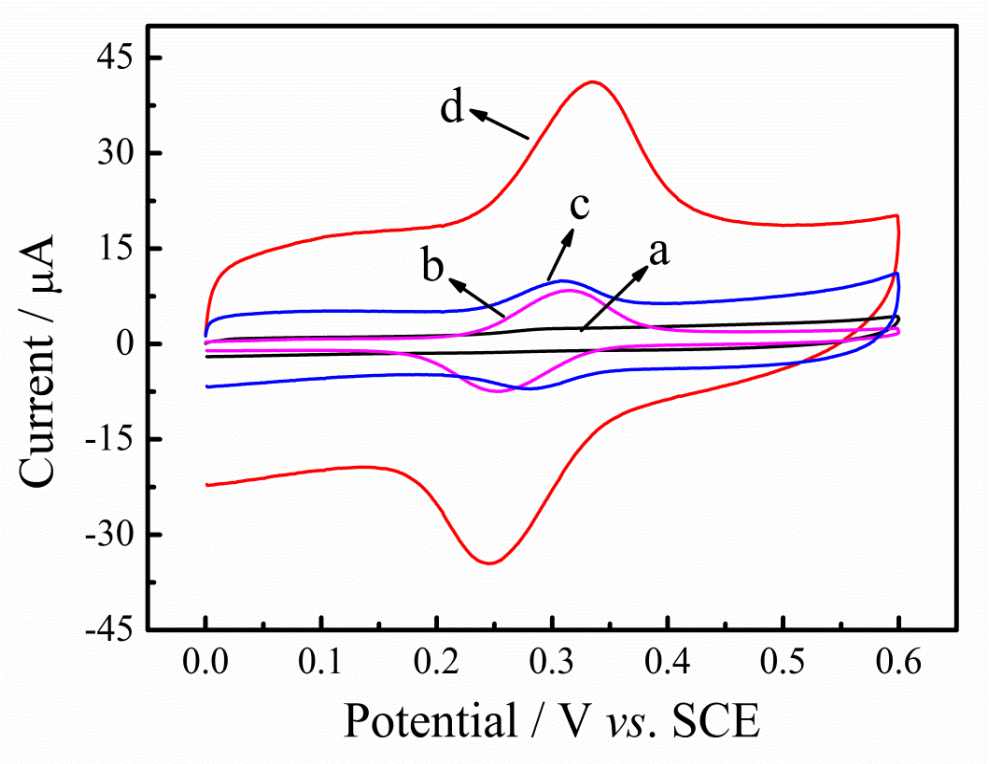

Figure 3. Cyclic voltammograms of 30 μM rutin in 0.1 M PBS (pH 7) at bare GCE (a), MWCNTs/GCE (b), ARGO/GCE (c) and MWCNTs/ARGO/GCE (d). Scan rate of 50 mV s^{-1}. Enrichment time: 40 s.

3.3 Optimization of the experimental conditions

3.4.1 Effect of enrichment time

Enrichment leads to more rutin molecules being absorbed on electrode surface and enhance sensitivity. Therefore, the dependence of oxidation peak current of rutin on enrichment time at MWCNTs/ARGO/GCE was investigated. MWCNTs/ARGO/GCE was immersed into 0.1 M PBS (pH 7.0) containing 30 μM rutin, and then stirred different time from 10 s to 70 s with an interval of 10 s before each detection. As can be seen from **Fig. 4**, the anodic peak current of rutin increased with the enrichment time from 10 s to 40 s, and then tended to be a constant. This indicated that enrichment time for 40 s led to saturated adsorption of rutin at MWCNTs/ARGO/GCE. Considering both work efficiency and sensitivity, 40 s was used in further experiments.

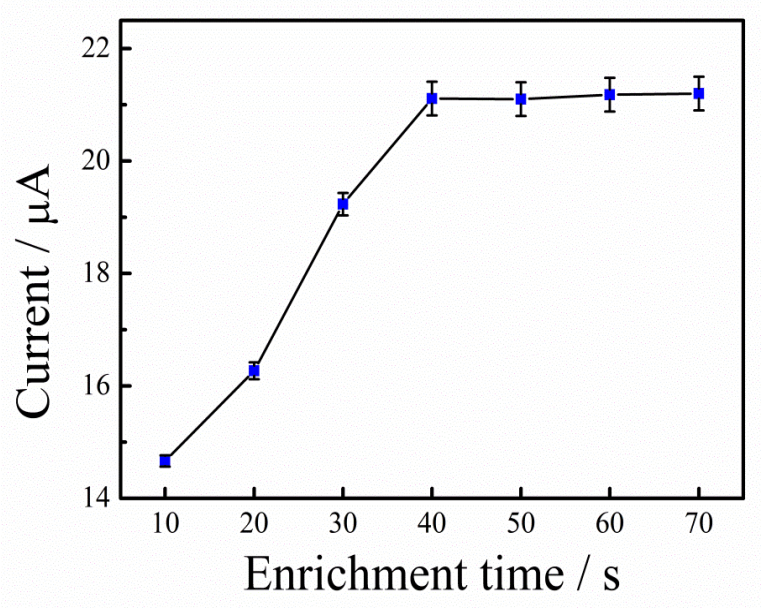

Figure 4. Variation of the peak currents with enrichment time in 0.1 M PBS (pH 7). rutin concentration: 30 μM. Scan rate: 50 mV s^{-1}.

3.4.2. Effect of pH values

The effect of pH value on the current responses of 30 μM rutin at MWCNTs/ARGO/GCE was investigated by changing pH value from 5 to 9 in 0.1 M PBS. As can be seen in **Fig. 5A**, with the increase of pH value, oxidation potential (E_{pa}) of rutin shifted toward negative values, indicating proton was involved in the electrode reaction. In addition, a good linear relationship between E_{pa} and pH value can be seen from **Fig. 5B**. The linear equation was E_{pa} = -0.064 pH + 0.900 (R^2 = 0.993). A slop of -0.064 mV pH^{-1} indicated the same number of electron and proton were involved in electrode reaction. Furthermore, it was also found that the oxidation peak exhibited highest current when the pH value was 7.0. Therefore, pH 7.0 was set for further experiment.

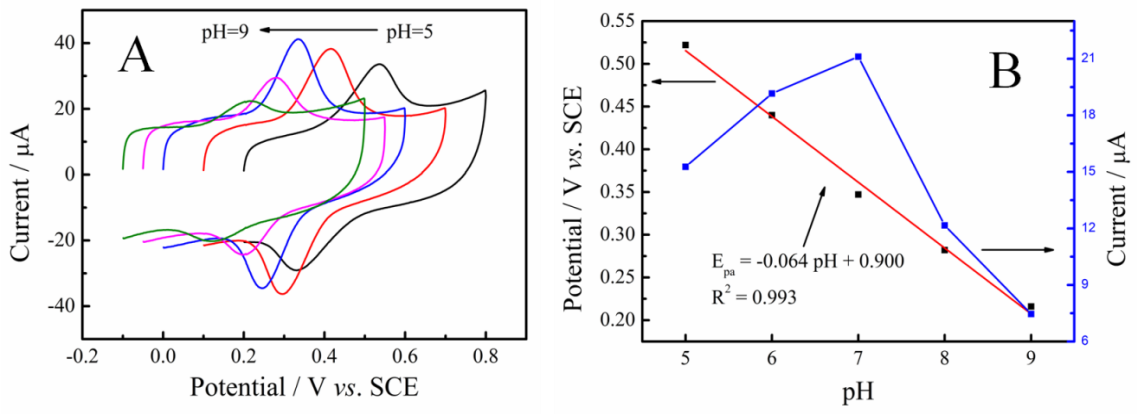

Figure 5. (A) CVs of MWCNTs/ARGO/GCE in PBS with different pH containing 30 μM rutin; (B) Effect of pH values on anodic peak potentials and anodic peak currents of rutin.

3.4.3 Effect of scan rates on the peak currents of rutin

In order to investigate the electrochemical reaction mechanism, the experiment of peak current responses of 30 μM rutin on MWCNTs/ARGO/GCE with different scan rate was carried out.

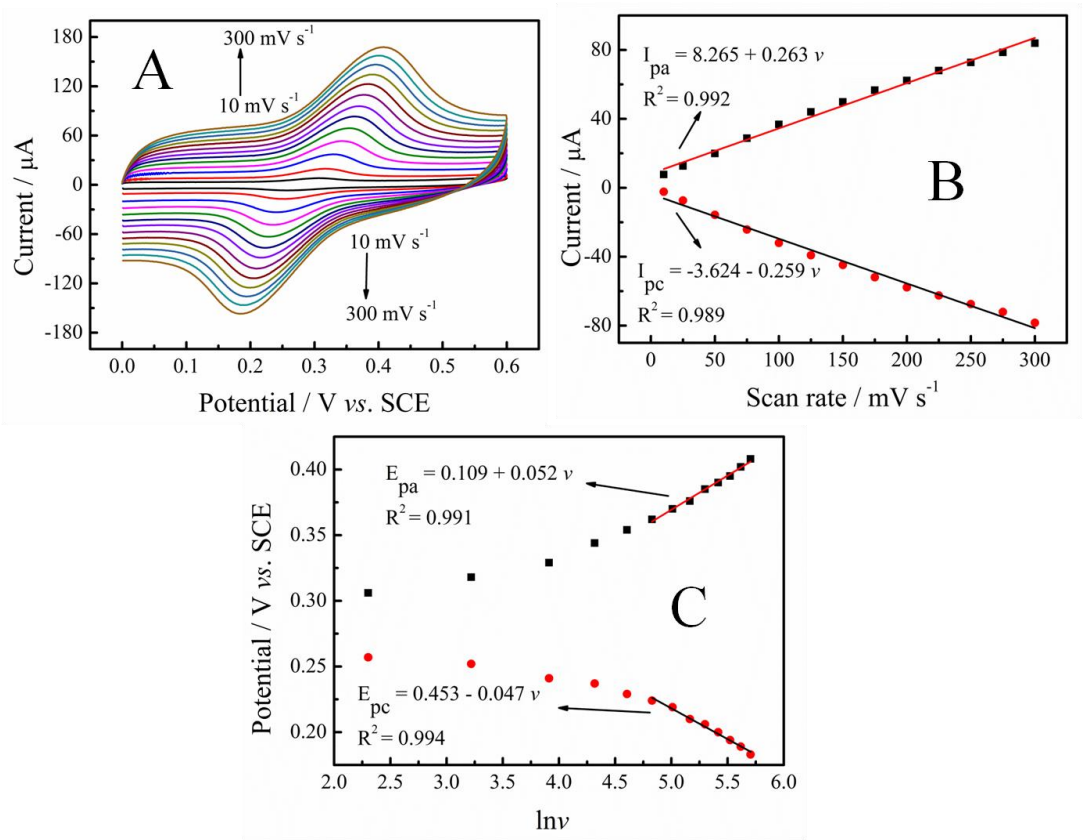

Figure 6. (A) Cyclic voltammograms of 30.0 μM rutin with different scan rates (v) at MWCNTs/ARGO/GCE in pH 0.1 PBS (pH 7) (from the inner to the outer are 10, 25, 50, 75, 100, 125, 150, 175, 200, 225, 250, 275, 300 mV s^{-1}, respectively.). (B) The relationship between redox peak currents and scan rates. (C) The relationship between redox peak potential and the natural logarithm of scan rates.

As shown in **Fig. 6A**, with the increase of the scan rate, the redox peak currents increased simultaneously, accompanied with an enlargement of the peak separation. And the peak currents of the redox peak currents varied linearly with the scan rates in a range from 10 to 300 mV s^{-1} (**Fig. 6B**), the linear regression equation can be expressed as I_{pa} = 8.265 + 0.263 *v* (R^2 = 0.992) and I_{pc} = -3.624 – 0.259 *v* (R^2 = 0.989), respectively. These behaviours illustrated that the redox of rutin on MWCNTs/ARGO/GCE was predominantly adsorption-controlled process [35].

Moreover, as shown in **Fig. 6C**, at higher scan rates, the anode (E_{pa}) and cathode (E_{pc}) peak potential had a linear relationship with the natural logarithm of scan rates (ln *v*). The regression equations were expressed as E_{pa} = 0.109 + 0.052 ln *v* and E_{pc} = 0.453 − 0.047 log *v* with R^2 = 0.991 and 0.994, respectively. According to Laviron's model [36], the slope of the line for E_{pa} and E_{pc} could be expressed as 2.3RT/n(1−α)F and -2.3RT/nαF, respectively. Therefore, the electron-transfer coefficient (α), electron-transfer number (n) and apparent rate constant (k_s) were calculated as 0.53, 2 and 0.26 s^{-1} respectively. These result indicated the fast electron-transfer process of rutin on the MWCNTs/ARGO/GCE.

3.4 Chronocoulometry

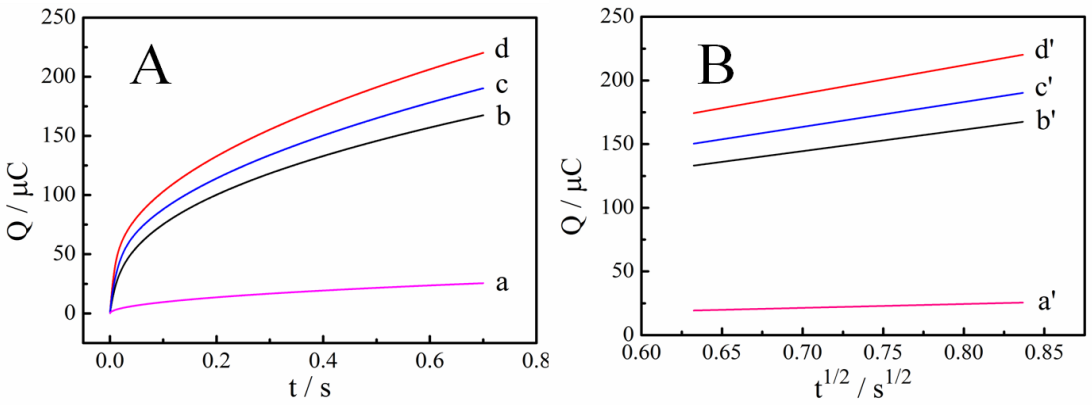

Figure 7. (A) Plot of Q-t curves of bare GCE (a), MWCNTs/GCE (b), ARGO/GCE (c) and MWCNTs/ARGO/GCE (d) in 0.1 mM $K_3[Fe(CN)_6]$ containing 1.0 M KCl. (B) Plot of Q-$t^{1/2}$ curves at bare GCE (a'), MWCNTs/GCE (b'), ARGO/GCE (c') and MWCNTs/ARGO/GCE (d').

The electrochemically effective surface areas (A) of bare GCE (**Fig. 7A**, curve a), MWCNTs/GCE (**Fig. 7A**, curve b), ARGO/GCE (**Fig. 7A**, curve c) and MWCNTs/ARGO/GCE (**Fig. 7A**, curve d) have been investigated. According to the previous literature [37], A can be determined by chronocoulometry using 0.1 mM $K_3[Fe(CN)_6]$ containing 1 M KCl as model complex, based on Anson equation:

$$Q(t) = 2nFAcD^{1/2}t^{1/2}/\pi^{1/2} + Q_{dl} + Q_{ads}$$

where Q_{ads} is Faradic charge, Q_{dl} is double layer charge, which could be eliminated by background subtraction, D is diffusion coefficient, c is concentration of substrate and A is effective surface area of working electrode. Other symbols have their usual meanings. The linear regression

equation of Q-$t^{1/2}$ curves on GCE, MWCNTs/GCE,ARGO/GCE and MWCNTs/ARGO/GCE were Q (10^{-6} C) = -3.455 + 20.384 $t^{1/2}$ (R^2 = 0.999), Q (10^{-6} C) = 25.433 + 164.020 $t^{1/2}$ (R^2 = 0.999), Q (10^{-6} C) = -26.991+200.339$t^{1/2}$ (R^2 = 0.999) and Q (10^{-6} C) = 37.596 + 220.670 $t^{1/2}$ (R^2 = 0.999), respectively (**Fig. 7B**). Based on the slopes of the linear relationship between Q and $t^{1/2}$, A was calculated to be 0.068 cm^2 for bare GCE, 0.546 cm^2 for MWCNTs/GCE, 0.667 cm^2 for ARGO/GCE. While the A of MWCNTs/ARGO/GCE was 0.735 cm^2, over 10 times higher than that of bare GCE. These results indicated that MWCNTs/ARGO/GCE showed larger surface area, which could increase the electrochemical active site, enhance the electrochemical response and decrease the detection limit.

3.5 Determination of rutin

Under the optimal experimental conditions established above, calibration curves of rutin in PBS were measured by differential pulse voltammetry (DPV). As shown in **Fig. 8**, the oxidation peak current was positive correlation to the rutin concentrations in the range of 0.01–112 μM, and the detection limit was estimated to be 2 nM (S/N = 3). The linear equation was I = 0.0.349 + 1.118 c (R^2 = 0.990). Besides, a comparison between the proposed method and other electrochemical techniques for the detection of rutin was provided in **Table 1**. It can be seen that the detection of rutin on MWCNTs/ARGO/GCE can achieve wider linear range and lower detection limit. These comparison data further indicated that MWCNTs/ARGO/GCE exhibited a significant enhance electrochemical performance towards rutin.

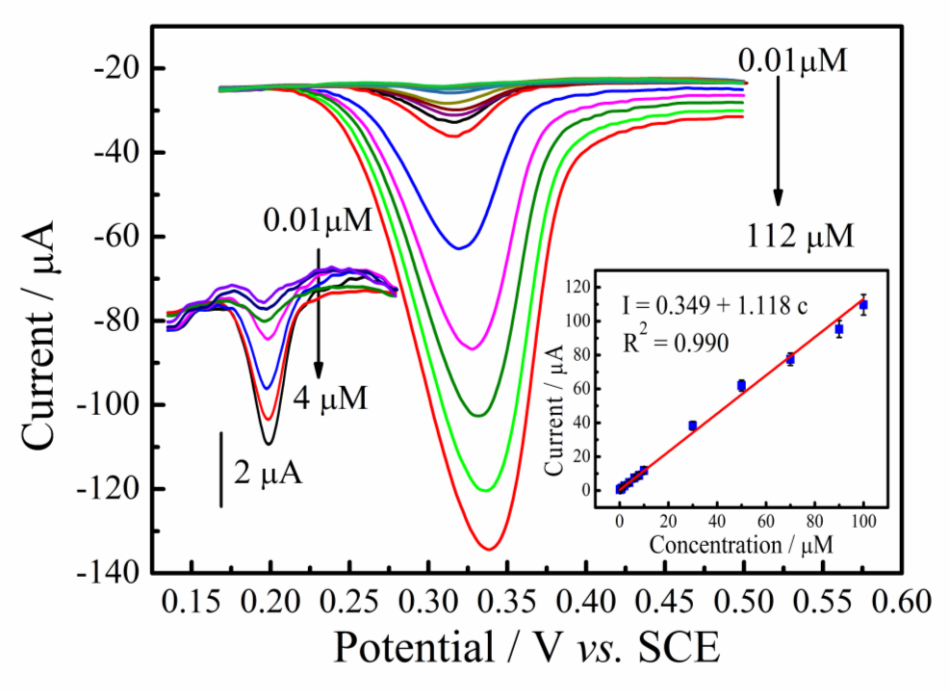

Figure 8. DPVs of 0.01, 0.06, 0.2, 0.8, 1, 4, 6, 8, 10, 30, 50, 70, 90 and 112μM rutin on MWCNTs/ARGO/GCE. Inset of Fig 7: plot of the oxidation peak currents against the concentrations of rutin. Other conditions are the same as Fig 3.

3.6 Long-term storage stability and interference study

Long-term storage stability experiment was carried out by using one electrode to detect 30 μM rutin each day. The electrode was stored in PBS after each measurement. Results indicated that no obvious change was noticed in peak current and peak potential after 5 days' detection. Only 4 % decrease of the current response was found after 20 days' detection, which demonstrated long-term stability of MWCNTs-rGNC/GCE.

Table 1. Comparison with other electrodes for the determination of rutin.

Modified electrodes	Linear range (μM)	Detection limit (μM)	References
[a]PYT/IL-CPE	0.5-100	0.358	[38]
[b]MWCNTs–CHIT/ABPE	0.02-10	0.01	[39]
[c]SWNT/Au	0.02-5	0.01	[11]
[d]ERG/CILE	0.07-100	0.024	[40]
[e]IL/CCE	0.3-100	0.09	[41]
[f]IL/CPE	0.04-10	0.01	[42]
[g]PVP/CPE	0.39-13	0.15	[43]
MWCNTs/ARGO/GCE	0.01-112	0.002	This work

[a]PYT/IL-CPE: pyridinium-typed ionic liquid modified carbon paste electrode;
[b]MWCNTs–CHIT/ABPE: multi-walled carbon nanotubes-chitosan modified acetylene black paste electrode;
[c]SWNT/Au: single-walled carbon nanotubes modified gold electrode;
[d]ERG/CILE: Electrochemical reduced graphene modified carbon ionic liquid electrode;
[e]IL/CCE: ionic liquid modified carbon ceramic electrode;
[f]IL/CPE: ionic liquid modified carbon paste electrode;
[g]PVP/CPE: poly(vinylpyrrolidone) modified carbon paste electrode.

Furthermore, possible interferences were investigated by introducing other species while the rutin concentration was fixed to 10 μM. The limit of potential interfering substances was defined as error-less than 5 % during the experiment. Results showed that 1000 fold of K^+, Na^+, Mg^{2+}, Ca^{2+}, Cu^{2+}, Fe^{3+}, Pb^{2+} showed that no significant interference on the current. In order to evaluate the effect of the presence of excipients commonly found in pharmaceutical formulations on the determination of rutin, 100 fold glucose, glycine, magnesium stearate, oxalic acid and citric acid were also investigated as potential sources of interference. None of these tested substances interfered in the determination of 10 μM rutin (signal change <5%). Such results indicated that the proposed analytical method had excellent anti-interference ability.

Table 2. Results for the determination of rutin in compound tablet samples.

samples	Specified (μM)	Detected (μM)	Added (μM)	Total found (μM)	Recovery (%)
1	3.02	3.00	0.5	3.44	98.29
2	3.02	2.99	1	4.13	103.51
3	3.02	3.02	5	7.98	99.50
4	3.02	3.04	8	11.24	101.81
5	3.02	2.98	12	21.11	100.62

3.7 Real sample analysis

In order to examine the proposed method in practical application, MWCNTs-rGNT/GCE was used to detect compound rutin tablets. Prior to analysis, the tablets were ground into fine powder with mortar, then accurately weighed. In order to prepare 1 mM rutin solution, the rutin power was transferred into 10 ml volumetric flask, then dissolved and brought to volume by 0.1 M PBS (pH 7.0). The sample analysis was carried out by DPV technique using a recovery test method. As can be seen in **Table 2**, the recovery of rutin was in the rang of 98.29–103.51 %, indicating that MWCNTs-rGNC/GCE can be successfully applied for the detection of rutin in real sample analysis.

4. CONCLUSION

In summary, MWCNTs/ARG nanoposite was prepared through a simple and efficient approach. ARGO not only acted as a dispersant which can effectively prevent aggregation of MWCNTs, but also provided excellent conductivity and large surface area. The composite combining the advantages of MWCNTs and ARGO possessed synergetic catalytic effect on the oxidation of rutin, and the significant increase in peak currents have greatly improved analytical performance of the prepared sensor. Under the optimized conditions, the MWCNTs/ARGO modified GCE exhibited good performance in terms of sensitivity, detection limit, response and linear calibration range for rutin detection. In addition, the proposed sensor also exhibited good repeatability, reproducibility and anti interference ability. These results indicate that the new MWCNTs/ARGO nanostructure is scientifically interesting and has great potential for use in sensors, nanoelectronics and other electrochemical applications.

ACKNOWLEDGEMENTS
We are grateful to the National Natural Science Foundation of China (51272096 and 51302117), the Natural Science Foundation of Jiangxi Province (20122BAB216011 and 20151BAB203018), Postdoctoral Science Foundation of China (2014M551857 and 2015T80688) and Postdoctoral Science Foundation of Jiangxi Province (2014KY14), Jiangxi Provincial Department of Education (GJJ13258) and the Science and Technology Landing Plan of Universities in Jiangxi province (KJLD14069 and KJLD12081) for their financial support of this work.

References

1. J. van der Geer, J.A.J. Hanraads, R.A. Lupton, *J. Sci. Commun*. 163 (2000) 51.
2. I. Kazuo, F. Takashi, K. Yasuji, *J. Chromatogr*. B 759 (2001) 161.
3. H.N.A. Hassan, B.N. Barsoum, I.H.I. Habib, *J. Pharm. Biomed. Anal*. 20 (1999) 315.
4. H.N.A. Hassan, B.N. Barsoum, I.H.I. Habib, *J. Pharm. Biomed. Anal*. 20 (1999) 315.
5. C.X. He, X.Y. Zhao, H.Z. Zhao, G.W. Zhao, *Anal. Lett*. 32 (1999) 2751.
6. Z. Legnerova, D. Satinsky, P. Solich, *Anal. Chim. Acta* 497 (2003) 165.
7. G.J. Volikakis, C.E. Efstathiou, *Talanta* 51 (2000) 775.
8. N.E. Zoulis, C.E. Efstathiou, *Anal. Chim. Acta* 320 (1996) 255.
9. J.L. He, Y. Yang, X. Yang, Y.L. Liu, Z.H. Liu, G.L. Shen, R.Q. Yu, *Sensor. Actuat*. B 114 (2006) 94.
10. J.W. Kang, X.Q. Lu, H.J. Zeng, H.D. Liu, B.Q. Lu, *Anal. Lett*. 35 (2002) 677.
11. B. Zeng, S. Wei, F. Xiao, F. Zhao, *Sensor. Actuat*. B 115 (2006) 240.
12. Y. Wei, G.F. Wang, M.G. Li, C. Wang, B. Fang, *Microchim. Acta* 158 (2007) 269.
13. A. Javey, J. Guo, Q. Wang, M. Lundstrom, H.J. Dai, *Nature* 424 (2003) 654.
14. L. Lu, X.. Zhu, X. Qiu, H. He, J. Xu, X. Wang, *Int. J. Electrochem. Sci.* 9 (2014) 8057-8066.
15. Z.C. Wu, Z.H. Chen, X. Du, J.M. Logan, J. Sippel, M. Nikolou, K. Kamaras, J.R. Reynolds, D.B. Tanner, A.F. Hebard, A.G. Rinzler, *Science* 305 (2004)1273.
16. Z. Wen, Q. Wang, Q. Zhang, J. Li, *Adv. Funct. Mater*. 17 (2007) 2772.
17. D.N. Futaba, K.Hata, T. Yamada, T. Hiraoka, Y. Hayamizu, Y. Kakudate, O. Tanaike, H. Hatori, M. Yumura, S. IiJima, *Nat. Mater*. 5 (2006) 987.
18. Y. Wu, K. Zhang, J. Xu, L. Zhang, L. Lu, L. Wu, T. Nie, X. Zhu, Y. Gao, W. Wen, *Int. J. Electrochem. Sci.* 9 (2014) 6594 – 6607.
19. J. Wang, M. Musameh, Y. Lin,*J. Am. Chem. Soc*. 9 (2003) 2408.
20. T. Casagrande, G. Lawson, H. Li, J. Wei, A. Adronov, I. Zhitomirsky, *Mater. Chem. Phys*. 111 (2008) 42.
21. L. Vaisman, H.D. Wagner, G. Marom, *Adv. Colloid Interface Sci.* 128 (2006) 37.
22. Y. Bai, I.S. Park, S.J. Lee, T.S. Bae, F. Watari, M. Uo, M.H. Lee, *Carbon* 49 (2011) 3663.
23. B. Vigolo, A. Pénicaud, C. Coulon, C. Sauder, R. Pailler, C. Journet, P. Bernier, P. Poulin, *Science* 290 (2000) 1331.
24. J. Wang, F. Wang, J. Yao, R. Wang, H. Yuan, K. Masakorala, M.M.F. Choi, *Colloids Surf. A* 417 (2013) 47.
25. A.R. Boccaccini, J. Cho, J.A. Roether, B.J.C. Thomas, E. Jane Minay, M.S.P. Shaffer, *Carbon* 44 (2006) 3149.
26. C. Du, N. Pan, *Nanotechnology* 17 (2006) 5314.
27. H. Park, J. Zhao, J.P. Lu, *Nano Lett*. 6 (2006) 916.
28. E. Heister, C. Lamprecht, V. Neves, C. Tîlmaciu, L. Datas, E. Flahaut, B. Soula, P. Hinterdorfer, H.M. Coley, S.R.P. Silva, *ACS Nano.* 4 (2010) 2615.
29. S.T. Nguyen, H.T. Nguyen, A. Rinaldi, N.P.V. Nguyen, Z. Fan, H.M. Duong, *Colloids Surf.* A 414 (2012) 352.
30. B. Vigolo, A. Pénicaud, C. Coulon, C. Sauder, R. Pailler, C. Journet, P. Bernier, P. Poulin, *Science* 290 (2000) 1331.
31. B. Vigolo, C. Coulon, M. Maugey, C. Zakri, P. Poulin, *Science* 309 (2005) 920.
32. W.B. Russel, D.A. Saville, W.R. Schowalter, Colloidal Dispersions, Cambridge University Press, 1992.
33. S. Cheemalapati, S. Palanisamy, V. Mani, S.M. Chen, *Talanta* 117 (2013) 297.
34. R. Wang, J. Sun, L. Gao, C. Xu, J. Zhang, *Chem. Commum*. 47 (2011) 8650.
35. T.V. Sathisha, B.E.K. Swamy, M. Schell, B. Eswarappa. *J. Electroanal. Chem*. 720 (2014) 1.
36. E. Laviron. *J. Electroanal. Chem*. 101 (1979) 19.

37. F. Anson, *Anal. Chem*. 36 (1964) 932.
38. W. Sun, M. Yang, Y. Li, Q. Jiang, S. Liu, K. Jiao, *J. Pharmaceut. Biomed*. 48 (2008) 1326.
39. P. Deng, Z. Xu, J. Li, *J. Pharmaceut. Biomed*. 76 (2013) 234.
40. F. Gao, X. Qi, X. Cai, Q. Wang, F. Gao, W. Sun, *Thin Solid Films*, 520 (2012) 5064.
41. T. Zhan, X. Sun, X. Wang, W. Sun, W. Hou, *Talanta*, 82 (2010) 1853.
42. Y. Zhang, J. Zheng, *Talanta* 77 (2008) 325.
43. A.C. Franzoi, A. Spinelli, I.C. Vieira, *J. Pharmaceut. Biomed*. 47 (2008) 973.